Inorganic Chemistry

Article

pubs.acs.org/IC

Photoinduced Dimerization Reaction Coupled with Oxygenation of a Platinum(II)–Hydrazone Complex

Atsushi Kobayashi,*[†] Daisuke Yamamoto,[†] Hiroyuki Horiki,[†] Kana Sawaguchi,[†] Takeshi Matsumoto,[†,∥] Kiyohiko Nakajima,[‡] Ho-Chol Chang,[§] and Masako Kato*[†]

[†]Department of Chemistry, Faculty of Science, Hokkaido University, North-10 West-8, Kita-ku, Sapporo 060-0810, Japan

[‡]Department of Chemistry, Aichi University of Education, Igaya, Kariya, Aichi 448-8542, Japan

[§]Department of Applied Chemistry, Faculty of Science and Engineering, Chuo University, 1-13-27 Kasuga, Bunkyo-ku, Tokyo 112-8551, Japan

S *Supporting Information*

ABSTRACT: Photoreactivities of Ni(II)– and Pt(II)–hydrazone complexes, [NiCl(L)] (**Ni1**) and [PtCl(L)] (**Pt1**), respectively [**HL** = 2-(diphenylphosphino)-benzaldehyde-2-pyridylhydrazone], were investigated in detail via UV–vis absorption, [1]H nuclear magnetic resonance (NMR) spectroscopy, and electrospray ionization time-of-flight (ESI-TOF) mass spectrometry; the two photoproducts obtained from the photoreaction of **Pt1** were also successfully identified via X-ray analysis. The absorption bands of the **Ni1** and **Pt1** complexes were very similar, centered around 530 nm, and were assigned as an intraligand charge transfer transition of the hydrazone moiety. The absorption spectrum of **Pt1** in a CH_3CN solution changed drastically upon photoirradiation (λ = 530 nm), whereas no change was observed for **Ni1**. [1]H NMR and ESI-TOF mass spectra under various conditions suggested that the photoexcited **Pt1*** reacts with dissolved dioxygen to form a reactive intermediate, and the ensuing dark reactions afforded two different products without any decomposition. In contrast to the simple photo-oxidation of **HL** to form a phosphine oxide **HL(P═O)**, the X-ray crystallographic analyses of the photoproducts clearly indicate the formation of a mononuclear Pt complex with the oxygenated hydrazone ligand (**Pt1O**) and a dinuclear Pt complex with the oxygenated and dimerized hydrazone ligand (**Pt2**). The photosensitized reaction in the presence of an $^1O_2$-generating photosensitizer, methylene blue (MB), also produced **Pt1O** and **Pt2**, indicating that the reaction between $^1O_2$ and ground-state **Pt1** is the important step. In a highly viscous dimethyl sulfoxide solution, **Pt1** was slowly, but quantitatively, converted to the mononuclear form, **Pt1O**, without the formation of the dinuclear product, **Pt2**, upon photoirradiation (and in the reaction photosensitized by MB), suggesting that this photoreaction of **Pt1** involves at least one diffusion-controlled reaction. On the other hand, the same complexes **Pt1O** and **Pt2** were also produced in the degassed solution, probably because of the reaction of the photoexcited **Pt1*** with the biradical character and H_2O.

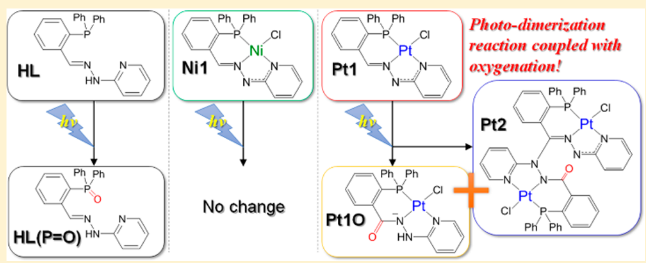

INTRODUCTION

Substituted hydrazones of the type $R_1R_2C{=}N\text{-}NHR_3$ (R_1, R_2, and R_3 = alkyl, aryl, acyl, etc.) are well-known functional organic compounds,[1−3] and the lone-pair electrons of the imine nitrogen allow them to coordinate to various metal ions.[4−8] Via the exploitation of the structural versatility of hydrazones, many metal complexes have been reported thus far, some of which exhibit interesting chromic behavior,[9−11] catalytic properties,[12−14] and biological activity.[15−17] One of the most characteristic features of metal–hydrazone complexes is the reversible protonation–deprotonation reaction.[18−21] We previously reported that the pK_a values of metal–hydrazone complexes depend strongly on the planarity of the coordinating hydrazone ligand,[20] which allowed the synthesis of vapochromic hydrogen-bonded proton transfer assemblies composed of metal–hydrazone complexes and anilic acids.[22,23] Consequently, coordination to metal ions produces remarkable effects not only on the molecular structure but also on the electronic state of the hydrazone.

In addition to the interesting properties of metal–hydrazone complexes, some organic hydrazones are also known to exhibit interesting photochromic behavior.[24−26] The typical example is 2-quinolylhydrazone reported by Wong et al. in 1973.[24] They reported that photochromism originates from the isomerization from the colorless *Z*-isomer to the colored *E*-isomer involving rotation around the C═N bond and the resulting change in the intramolecular hydrogen bonding motif. These observations have motivated our investigation of the photochemical reactivity of metal–hydrazone complexes. Considering the fact that geometrical changes of the hydrazone ligand should be strictly limited by coordination to the metal ion, photochemical

Received: November 20, 2013
Published: February 17, 2014

   dx.doi.org/10.1021/ic402879g | Inorg. Chem. 2014, 53, 2573−2581

reactions of the metal−hydrazone complexes are expected to be largely different from those of purely organic hydrazones. Nevertheless, there are only a few existing reports about the photochemical reactions of metal−hydrazone complexes. Therefore, in this study, we investigate the photoreactivity of metal−hydrazone complexes bearing d^8 metal ions, [MCl(L)] [Scheme 1; **HL** = 2-(diphenylphosphino)benzaldehyde-2-pyridylhydrazone; M = Ni(II) or Pt(II)], demonstrating the unique photodimerization reaction of the **Pt1** complex coupled with the oxidation of the hydrazone moiety to form both the oxygenated form, **Pt1O**, and the dimerized form, **Pt2**. On the other hand, the **Ni1** complex does not exhibit any photoreaction, and the **HL** ligand itself is photoconverted to the phosphine oxide **HL(P═O)** without any change in the hydrazone moiety. The key step is the reaction between the $^1O_2$ generated by the transfer of excitation energy from photoexcited **Pt1*** and ground-state **Pt1**. In addition, we present the successful selective and quantitative synthesis of the oxygenated form (**Pt1O**) by using highly viscous dimethyl sulfoxide (DMSO) as the reaction solvent.

Scheme 1. Structural Representation of Hydrazone Ligands HL, HL(P═O), Metal−Hydrazone Complexes (Ni1 and Pt1), and Photoproducts (Pt1O and Pt2) Obtained from the Photoreaction of Pt1

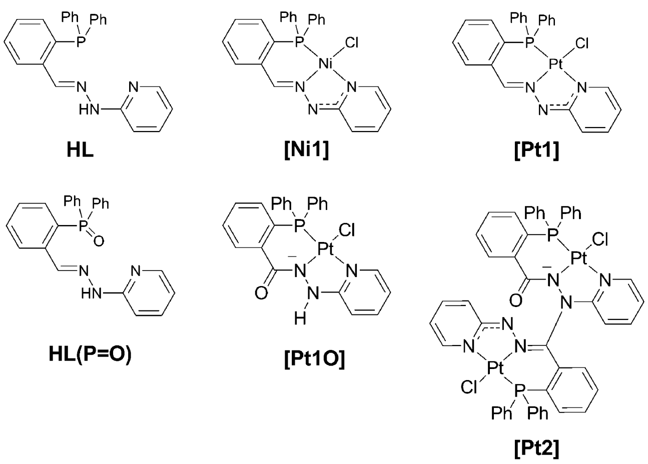

EXPERIMENTAL SECTION

Syntheses. All commercially available starting materials were used as received, and the solvents for the syntheses were used without further purification. Unless otherwise stated, all manipulations were performed in air and in a dark room. 2-(Diphenylphosphino)-benzaldehyde, 2-hydrazinopyridine, and $NiCl_2{\cdot}6H_2O$ were purchased from Wako Pure Chemical Industries, Ltd. K_2PtCl_4 was purchased from Tanaka Kikinzoku Kogyo K.K. The hydrazone ligand (**HL**)[27] and the Pt(II)−hydrazone complex [PtCl(L)] (**Pt1**)[20] were prepared according to the published methods.

HL(P═O). **HL** (51.9 mg, 0.136 mmol) in CH_2Cl_2 (20 mL) was combined with a 30% H_2O_2 aqueous solution (5.0 mL) in an ice bath. After being continuously stirred for 2 h at 273 K, the reaction solution was washed with two 10 mL aliquots of water and three aliquots of a saturated NaCl aqueous solution (10 mL) to remove unreacted H_2O_2. The obtained organic phase was dried over $MgSO_4$, and the solvent was removed to dryness under reduced pressure to afford a pale-yellow solid. This solid was washed with water (10 mL) and collected by filtration. Yield: 28.8 mg, 53%. Elemental analysis calculated for $C_{24}H_{20}N_3OP$: C, 72.53; H, 5.07; N, 10.57. Found: C, 72.15; H, 4.98; N, 10.09. ^{1}H NMR (DMSO-d_6): δ 11.09 (s, 1H), 8.65 (s, 1H), 8.22 (dd, 1H), 8.08 (d, 1H), 7.54−7.67 (m, 13H), 7.37 (t, 1H), 7.19 (d, 1H), 7.06 (dd, 1H), 6.76 (t, 1H).

*[NiCl(L)] (**Ni1**).* $NiCl_2{\cdot}6H_2O$ (35.8 mg, 0.150 mmol) in CH_3CN (7.5 mL) was combined with the CH_3CN suspension (7.5 mL) of Hpbph (57.2 mg, 0.150 mmol). After the solution had been continuously stirred for 30 min at room temperature, triethylamine (210 μL, 1.5 mmol) was added to the obtained orange suspension; the suspension immediately became purple. This reaction mixture was refluxed for 4 h and then filtered to remove the white precipitate. The filtrate was evaporated to dryness under reduced pressure to afford a red solid. This red solid was washed with water (10 mL) and collected by filtration. Yield: 41.6 mg, 58%. Elemental analysis calculated for $C_{24}H_{19}N_3PClNi$: C, 60.74; H, 4.04; N, 8.85. Found: C, 61.02; H, 4.28; N, 8.70. ^{1}H NMR ($CDCl_3$): δ 8.01 (s, 1H), 7.87 (d, 1H), 7.73−7.83 (m, 4H), 7.40−7.56 (m, 8H), 7.06−7.20 (m, 3H), 6.62 (d, 1H), 6.26 (t, 1H). ESI-TOF mass (positive ion, CH_3CN): m/z 474.06 ([**Ni1** + H]$^+$).

*Photo-oxygenated and Photodimerized Pt(II)−Hydrazone Complexes [PtCl(HL=O)] (**Pt1O**) and [Pt_2Cl_2(L-L═O)] (**Pt2**).* These two complexes were obtained from the following photoreaction and then separated. A CH_3CN solution (120 mL) of **Pt1** (105.8 mg, 0.173 mmol) in a 200 mL Pyrex glass flask was immersed in a water bath maintained at 25 °C and then irradiated for 13 h using a 500 W xenon light source (USHIO Optical ModuleX SX-UI500XQ) with a long-pass filter (λ > 500 nm). The obtained suspension was evaporated to dryness under reduced pressure to afford a mixture of yellow and orange solids. This mixture was purified by column chromatography on silica gel (eluent, 3:7 *n*-hexane/ethyl acetate). The yellow and orange bands were collected separately, and the solvent was removed under reduced pressure to afford yellow and orange crystalline solids, respectively. These products were identified as **Pt1O** and **Pt2** complexes, respectively, via ^{1}H NMR measurements (see below). Each of the obtained solids was washed with hexane (10 mL) and collected by filtration. Single crystals suitable for X-ray structural determination were obtained by slow evaporation of the solution purified by silica gel column chromatography. Yield for the yellow solid (**Pt1O**): 4.2 mg, 3.9% based on **Pt1**. Elemental analysis calculated for $C_{24}H_{19}ClN_3OPPt$ (**Pt1O**): C, 45.98; H, 3.05; N, 6.70. Found: C, 46.10; H, 3.18; N, 6.50. ^{1}H NMR (DMSO-d_6): δ 11.60 (s, 1H), 8.63 (dd, 1H), 8.38−8.42 (m, 1H), 7.73 (t, 1H), 7.66 (t, 1H), 7.47−7.61 (m, 11H), 7.32 (d, 1H), 7.14 (dd, 1H), 6.68 (t, 1H). ESI-TOF mass (positive ion, CH_2Cl_2): m/z 626 ([**Pt1O** − H]$^+$). Yield for the orange solid (**Pt2**): 40.9 mg, 38.3% based on **Pt1**. Elemental analysis calculated for $C_{48}H_{36}Cl_2N_6OP_2Pt_2{\cdot}H_2O$ (**Pt2**$\cdot H_2O$): C, 45.98; H, 3.05; N, 6.70. Found: C, 45.99; H, 3.12; N, 6.71. ^{1}H NMR (DMSO-d_6): δ 8.80 (m, 1H), 8.03 (m, 2H), 7.80 (m, 2H), 7.40−7.70 (m, 23H), 7.05−7.40 (m, 4H), 7.03 (t, 1H), 6.60 (t, 1H), 6.45 (t, 1H), 6.40 (t, 1H). ESI-TOF mass (positive ion, CH_3CN): m/z 1236.07 ([**Pt2** + H]$^+$).

Single-Crystal X-ray Diffraction Measurements. All single-crystal X-ray diffraction measurements were performed using a Rigaku Mercury CCD diffractometer with graphite-monochromated Mo Kα radiation (λ = 0.71069 Å) and a rotating anode generator. Each single crystal was mounted on MicroMount with paraffin oil. The crystal was cooled using a N_2-flow-type temperature controller. Diffraction data were collected and processed using CrystalClear.[28] Structures were determined by the direct method using SIR-2004.[29] Structural refinements were performed by full-matrix least squares using SHELXL-97.[30] Non-hydrogen atoms were refined anisotropically; hydrogen atoms bound to oxygen atoms were refined isotropically, and other hydrogen atoms were refined using the riding model. All calculations were performed using the Crystal Structure crystallographic software package.[31] The crystallographic data obtained for each complex are summarized in Table 1.

Measurements. UV−vis absorption and luminescence spectra of the complexes were recorded on a Hitachi U-3000 spectrophotometer and a Jasco FP-6600 spectrofluorometer, respectively. Prior to the luminescence measurements, the sample solutions were deoxygenated by the freeze−pump−thaw method. ^{1}H NMR spectra were recorded on a JEOL JNM-EX270 FT-NMR system with chemical shifts (in

Table 1. Crystal Parameters and Refinement Data

	Pt1O	Pt2
T (K)	293(1)	130(1)
formula	$C_{24}H_{19}ClN_3OPPt$	$C_{48}H_{36}Cl_2N_6OP_2Pt_2$
formula weight	626.95	1235.89
crystal system	monoclinic	monoclinic
space group	$C2/c$	$P2_1/n$
a (Å)	29.907(8)	15.241(5)
b (Å)	7.467(2)	11.609(4)
c (Å)	20.066(5)	25.365(8)
α (deg)	90	90
β (deg)	100.851(4)	98.718(3)
γ (deg)	90	90
V (Å^3)	4401(2)	4436(3)
Z	8	4
D_{cal} (g cm^{-3})	1.892	1.850
no. of reflections collected	17504	45115
no. of unique reflections	4936	11231
goodness of fit	1.053	1.150
R [$I > 2.00\sigma(I)$]	0.0397	0.0676
R_W	0.1212	0.2046

parts per million) relative to tetramethylsilane. Elemental analyses and electrospray ionization time-of-flight (ESI-TOF) mass spectrometry were performed using a MICRO CORDER JM 10 analyzer and a JEOL JMS-T100LP spectrometer, respectively, at the Analysis Center of the Hokkaido University. Photoirradiation of sample solutions was conducted in a dark room using the 150 W xenon light source of the Shimadzu RF-5300PC fluorophotometer or a USHIO (Optical ModuleX) xenon lamp (SX-UI500XQ) combined with a long-pass filter (λ > 500 nm) purchased from Asahi Spectra Co. The reaction solution was bubbled with Ar or O_2 for 1 h to be degassed or saturated by O_2 before each photolysis experiment. The solution was placed in a quartz cell with a 1 cm path length for UV–vis absorption measurement or in a NMR quartz tube (5 mm) for ^{1}H NMR spectral measurements.

■ RESULTS AND DISCUSSION

Absorption and Emission Properties of Metal–Hydrazone Complexes. Figure 1 shows the UV–vis absorption and luminescence spectra of the **Ni1** and **Pt1** complexes in a CH_3CN solution at room temperature compared with the absorption spectrum of the **HL** ligand. As previously reported, the **Ni1** and **Pt1** complexes showed relatively intense intraligand charge transfer (ILCT) transition bands at 533 and 530 nm, respectively, whereas the spectrum of hydrazone ligand **HL** showed only a strong absorption band in the UV region at 335 nm.[20] This difference suggests that the complexation reaction involving the deprotonation of the hydrazone moiety had a large effect on the electronic state of the hydrazone ligand. In addition, a weak absorption band at ~645 nm was observed only in the case of the **Ni1** complex and could be assigned as the d–d transition of the Ni^{2+} center. We also found that the **Pt1** complex exhibited red emission centered around 600 nm, whereas **Ni1** was found to be a nonemissive complex. The red emission of **Pt1** is tentatively assigned as the ^{3}ILCT emission, whereas the low-lying d–d transition state would afford facile nonemissive deactivation of the **Ni1** complex.

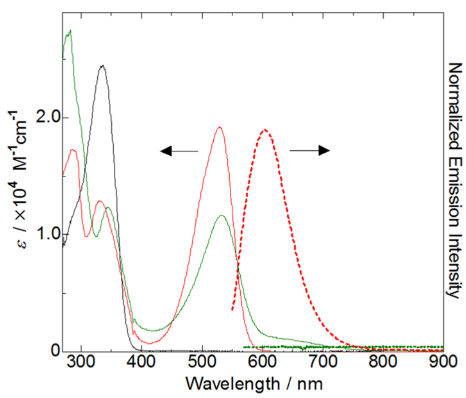

Figure 1. Comparison of UV–vis absorption and luminescence spectra of **Ni1** (green) and **Pt1** (red) in an anhydrous CH_3CN solution with the absorption spectrum of **HL** (black). Solid and dotted lines show absorption and luminescence spectra, respectively.

Photoreactions of Metal(II)–Hydrazone Complexes. As mentioned in the Introduction, we have previously reported the variation of the UV–vis spectral profile of **Pt1** under various pH conditions in methanol and found that the absorption band centered around 530 nm, attributed to the ILCT transition, disappeared upon protonation of the hydrazone moiety.[20] It was also found that the color of the solution and the emission of **Pt1** gradually changed under photoirradiation without the addition of acids. This change motivated us to investigate the photoreactivity of metal(II)–hydrazone complexes. UV–vis absorption spectra of the **Ni1** and **Pt1** complexes were acquired under photoirradiation in the solution state. Figure 2 shows the spectral changes of the UV–vis absorption in 0.1 mM CH_3CN solutions under photoirradiation. The wavelength of the incident light corresponded to the energy of the ILCT transition and was controlled using the 150 W xenon lamp and diffraction grating of the Shimadzu RF-5300PC fluorophotometer. Interestingly, the spectrum of **Pt1** changed drastically and rapidly upon irradiation, and the color of the solution changed from red to clear yellow. The original ILCT band of **Pt1** almost disappeared after photoirradiation for ~4 h, and a new weak absorption band appeared at 398 nm. The spectrum of **Pt1** obtained after irradiation for 2 h was similar to that of the protonated form, $[PtCl(HL)]^+$, in the low-pH solutions, implying that the hydrazone moiety could react with certain molecules upon irradiation. In contrast to the drastic change observed for **Pt1**, the spectrum of **Ni1** remained largely unchanged under light irradiation. This is plausibly attributed to the fast deactivation of the photoexcited

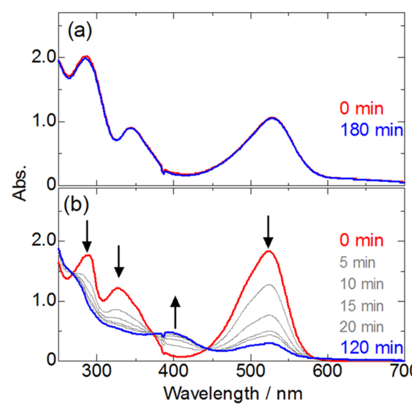

Figure 2. Changes in the UV–vis spectral profile of (a) **Ni1** and (b) **Pt1** in 0.1 mM CH_3CN degassed solutions under photoirradiation (λ_{irr} values of 532 and 529 nm for **Ni1** and **Pt1**, respectively).

state through the low-lying d−d states of the Ni^{2+} center. Furthermore, it was found that the photoreaction of **Pt1** was strongly affected by the presence of dissolved oxygen in the reaction solvent. Figure 3 shows the irradiation time dependence of the absorbance of the ILCT band of **Pt1** in a 0.1 mM CH_3CN solution. The absorbance of the ILCT band was found to decrease 4 times more rapidly in the O_2-saturated solutions than in the deoxygenated solutions. Moreover, the spectra observed under these conditions were almost identical to each other (Figure S1 of the Supporting Information), indicating that the concentration of dissolved oxygen and/or water in the reaction solutions does not affect the photoproduct itself but affects the reaction rate. In contrast, the rate of reduction of the ILCT band intensity depends slightly on the amount of water in the CH_3CN solvent. This result suggests that the photoreaction of **Pt1** probably involves reaction with the O_2 molecule.

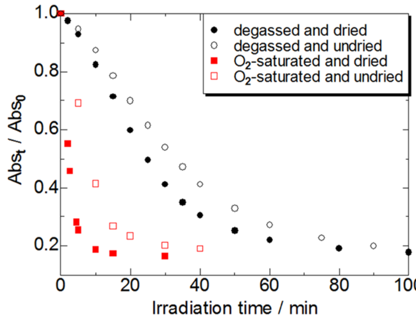

Figure 3. Plot of changes in the absorbance of the ILCT band of **Pt1** (λ_{abs} = 530 nm) in a 0.1 mM CH_3CN solution vs photoirradiation time. Abs_0 and Abs_t are the absorbance of the ILCT band before light irradiation and at irradiation time t, respectively.

To obtain further insight into the photoreaction of **Pt1**, the ^{1}H NMR and ESI-TOF mass spectral changes of complex **Pt1** upon light irradiation were monitored. Figure 4 shows the ^{1}H NMR spectral change of **Pt1** in a CD_3CN solution. Photoirradiation was conducted by using the 500 W xenon lamp (USHIO Optical ModuleX) combined with the long-pass filter (λ > 500 nm). Prior to irradiation, the typical singlet peak assigned to the proton bonded to the imine carbon was clearly observed at 8.31 ppm, and the three characteristic protons bound to the pyridine ring were also observed at 6.36, 6.82, and 8.21 ppm. The main peak observed in the ESI-TOF mass spectra of **Pt1** prior to photoirradiation corresponded exactly to the molecular mass of the protonated form, $[PtCl(HL)]^+$ (**Pt1H$^+$**, m/z 612) (Figure S2 of the Supporting Information). Upon irradiation, the magnitudes of the original NMR signals of **Pt1** decreased rapidly, and several new peaks appeared simultaneously at 6.70, 7.18, 8.55, 8.68, 8.70, and 10.34 ppm. A drastic change was also observed in the ESI-TOF mass spectrum. The original peak of **Pt1H$^+$** (m/z 612) almost disappeared, and several new peaks appeared (Figure S3 of the Supporting Information). The main peak after photoirradiation was observed at approximately twice the original ratio (m/z 1236), suggesting that certain dimerized species were formed upon photoirradiation. The small deviation from the exact value of twice the original mass to charge ratio might be due to the reaction with O_2 or water. It may be interesting to note that the second peak in the region above the original mass was observed at m/z 626. The difference between the new mass and the original mass is also close to the mass of the oxygen atom, implying that photo-oxidation reactions may have occurred. Fortunately, isolation of the two different photoproducts by silica gel column chromatography [7:3 (v:v) ethyl acetate/n-hexane (Experimental Section)] and crystallization of these complexes was successful. Single-crystal X-ray structural analyses clearly revealed that the two isolated complexes were oxygenated mononuclear complex **Pt1O** and oxygenated dinuclear form **Pt2** (Crystal Structures of Photoproducts). In addition, the characteristic ^{1}H NMR signals of **Pt1O** (δ 6.70, 8.55, 8.68, and 10.34) and **Pt2** (δ 7.18 and 8.70) were also observed for the photoproducts obtained from the photoirradiation of the CH_3CN solution of **Pt1**, as shown in Figure 4. From the ^{1}H NMR spectrum after a 2 min photoirradiation, the **Pt1O**:**Pt2** molar ratio was estimated to be ∼3:1 under the stated reaction conditions. Thus, the photoreaction of **Pt1** should involve two different chemical reactions: (1) oxygenation of the hydrazone moiety and (2) dimerization between two metal−hydrazone molecules. Considering the fact that the UV−vis spectra of both **Pt1O** and **Pt2** were hardly changed by photoirradiation with the same wavelength, the oxygenation and dimerization reactions are believed to occur competitively. We also investigated the photoreaction of ligand **HL** in a DMSO-d_6 solution and found a contrasting result; the phosphine moiety was oxidized by photoirradiation (λ > 310 nm) to form phosphine oxide **HL(P═O)** without any change in the hydrazone moiety (Figure S4 of the Supporting Information). This difference suggests that coordination of the hydrazone ligand to the Pt(II) ion not only protects the phosphine group from oxidation by dissolved dioxygen but also changes the photoexcited state.

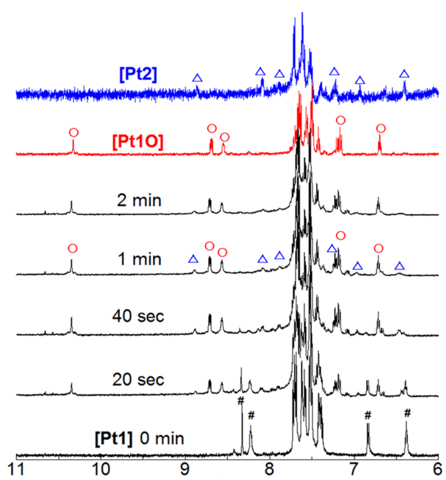

Figure 4. Changes in ^{1}H NMR spectral profile of **Pt1** (aromatic region) in a CD_3CN solution under photoirradiation (λ_{irr} > 500 nm) at room temperature. Red and blue lines show the spectra of **Pt1O** and **Pt2** complexes, respectively, purified by column chromatography. Symbols #, ○, and △ indicate characteristic signals of starting complex **Pt1**, oxygenated form **Pt1O**, and dimerized form **Pt2**, respectively.

Many organic compounds are oxidized by singlet oxygen ($^1O_2$) that can be generated by the photoexcitation of organic dyes.[32,33] To determine whether the reaction between $^1O_2$ and **Pt1** occurs, the photosensitization reaction with methylene blue (MB), a well-known organic dye for efficiently producing $^1O_2$ upon irradiation with red light, was investigated.[33] An intense π−π* absorption band was observed at 655 nm, which is longer than the wavelength of the ILCT absorption of **Pt1** (530 nm).

dx.doi.org/10.1021/ic402879g | Inorg. Chem. 2014, 53, 2573−2581

Thus, irradiation with red light at 660 nm allowed selective excitation of MB to generate $^1O_2$ in the reaction solution. Figure 5 shows the changes in the UV−vis spectra of a 0.1 mM

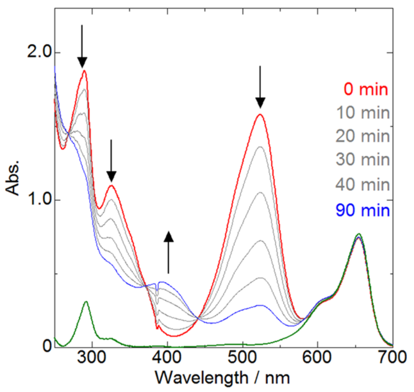

Figure 5. Changes in the UV−vis spectral profile of **Pt1** in a 0.1 mM CH_3CN O_2-saturated solution with 0.01 mM methylene blue (MB) as a photosensitizer under irradiation at 660 nm. The green line shows the absorption spectrum of MB.

Pt1/CH_3CN O_2-saturated solution containing 0.01 mM MB as the $^1O_2$-generating photosensitizer under red light irradiation (λ_{irr} = 660 nm). Interestingly, the ILCT band of **Pt1** gradually disappeared, and a new absorption band simultaneously appeared at 395 nm. The $\pi-\pi^*$ absorption band of MB remained the same, indicating that the photoexcited MB* generates only highly reactive $^1O_2$ by the transfer of energy to the ground-state $^3O_2$; MB itself does not react with **Pt1**. This spectral change is identical to the change observed in the direct excitation of **Pt1**, as shown in Figure 2b. In addition, the change in the ^1H NMR spectra for the solution containing MB also indicates the formation of two complexes, **Pt1O** and **Pt2** (Figure S5 of the Supporting Information). Thus, it is evident that the $^1O_2$ generated by the transfer of energy from MB* reacts with **Pt1** in the ground state to form a reaction intermediate. In contrast, the UV−vis spectral change and ESI-TOF mass spectrometry for the products obtained from the MB-photosensitized reaction of **Ni1** in an O_2-saturated CH_3CN solution revealed that **Ni1** was decomposed rapidly within 10 min by the reaction with $^1O_2$ (see Figures S6 and S7 of the Supporting Information). It might be because the **Ni1** would be oxidized more easily than **Pt1**. We also confirmed that the photoreaction of **Pt1** in the CH_3CN solution was effectively suppressed by the presence of 10 equiv of DABCO (1,4-diazabicyclo[2.2.2]octane), a well-known $^1O_2$ quencher (see Figure S8 of the Supporting Information), suggesting that the reaction between **Pt1** and $^1O_2$ is one important step for the formation of **Pt1O** and **Pt2**. It should be noted that the change in the UV−vis spectrum in the case of the photosensitization reaction with MB occurred more slowly than that by the direct photoexcitation of **Pt1**. This may be reasonable because $^1O_2$ should make contact and react with **Pt1** within the lifetime of the excited state (~60 μs),[34] which is a diffusion-controlled process. Thus, the photoreaction of **Pt1** to form two different complexes, **Pt1O** and **Pt2**, should be triggered by the reaction between the photoexcited **Pt1*** in the ^{3}ILCT transition state and dissolved oxygen to form $^1O_2$ by energy transfer; dark reaction between these species would produce an intermediate. The important step in generating either **Pt1O** or **Pt2** should be the contact between the intermediate and the second **Pt1** molecule. If the intermediate can react with the second **Pt1** molecule, the dimerization reaction would occur to form **Pt2**. In this case, the solvent should play an important role in the control of the **Pt1O**:**Pt2** ratio in the photoreaction of **Pt1**. To clarify the effect of the solvent, the changes in the ^1H NMR spectral profile of **Pt1** in a DMSO-d_6 solution were monitored. As shown in Figure 6, the spectrum acquired after irradiation

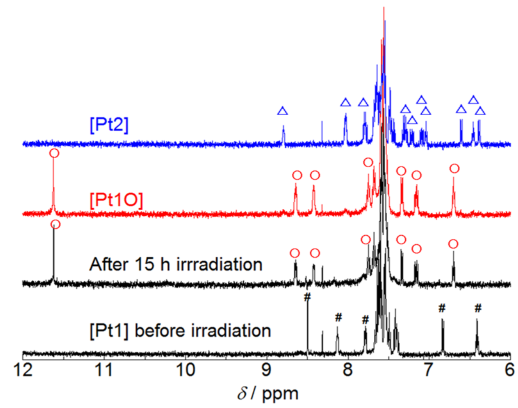

Figure 6. Changes in the ^1H NMR spectral profile of **Pt1** (aromatic region) in a DMSO-d_6 solution under photoirradiation (λ_{irr} > 500 nm) at room temperature. Red and blue lines show spectra of **Pt1O** and **Pt2** complexes, respectively, purified by column chromatography. Symbols #, ○, and, △ indicate characteristic signals of starting complex **Pt1**, oxygenated form **Pt1O**, and dimerized form **Pt2**, respectively.

for 15 h was almost identical to the spectrum of **Pt1O**, and no signals derived from **Pt2** were observed. This result is reasonable because the viscosity of DMSO is 7 times higher (η = 2.00 cP at 298 K) than that of CH_3CN (η = 0.34 cP at 298 K). In such a highly viscous solution, the reaction intermediate generated from the reaction of $^1O_2$ and **Pt1** could not react with the second **Pt1**, resulting in the formation of mononuclear complex **Pt1O**. In addition to the high solvent viscosity, the DMSO solvent may act as a trapping agent of a nucleophilic peroxidic reaction intermediate.[35] Likewise, an electrophilic peroxidic intermediate could have been trapped by dimethyl sulfide (DMS) which may be present as an impurity in the DMSO solvent. In fact, the photoreaction of **Pt1** in the CD_3CN solution was strongly suppressed by the presence of DMS (see Figure S9 of the Supporting Information). The MB-photosensitized reaction in a DMSO solution was also evaluated; it was found that only mononuclear complex **Pt1O** was formed (Figure S10 of the Supporting Information). The reaction rate in DMSO was found to be much lower than that in CH_3CN, which is consistent with the fact that the reaction between photoexcited **Pt1*** and dissolved oxygen is also diffusion-controlled.

A plausible mechanism for the photoreaction of **Pt1** is summarized in Scheme 2. The results of several spectroscopic evaluations of the photochemical reaction of **Pt1** in an O_2-saturated CH_3CN solution presented here clearly indicate that this reaction is triggered by the transfer of photoexcitation energy from **Pt1*** in the ^{3}ILCT transition state to the ground-state $^3O_2$ to generate reactive $^1O_2$ (route A, first step). This $^1O_2$ possibly reacts with the electron-rich C═N bond in the hydrazone group because of its electrophilic nature. Although we have not determined the detailed molecular structure of the reaction intermediate, one possible candidate is the hydro-

dx.doi.org/10.1021/ic402879g | Inorg. Chem. 2014, 53, 2573−2581

Scheme 2. Plausible Mechanism for the Photochemical Reaction of Pt1

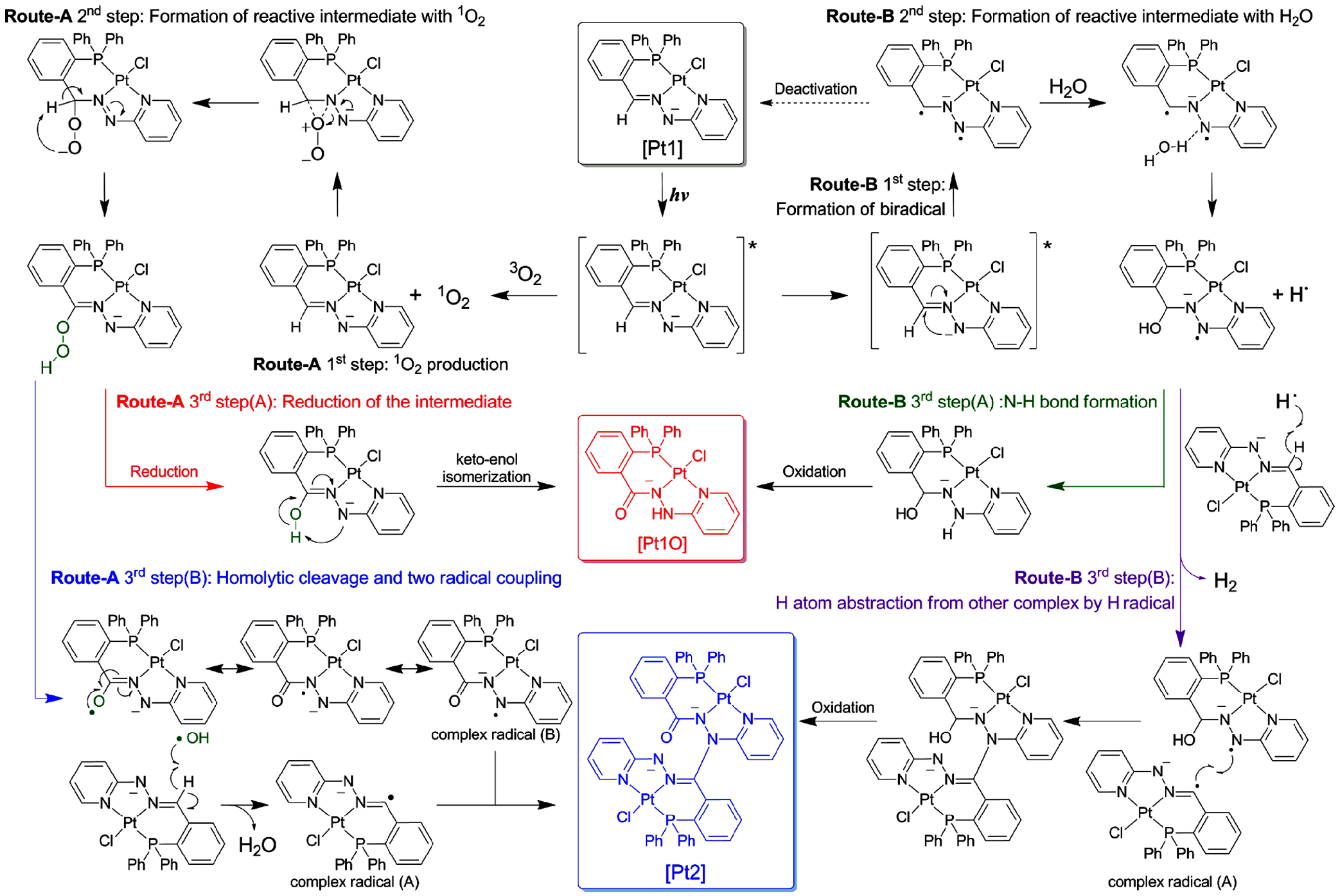

peroxide complex shown at the end of the second step of route A. If this hydroperoxide group is reduced to the hydroxyl group, keto−enol isomerization could produce the mononuclear **Pt1O** complex [route A, third step (A)]. On the other hand, if homolytic cleavage of the O−O bond occurs, two different hydroxyl radicals, the simple hydroxyl radical and the complex radical (B) in which the radical is delocalized in the hydrazone moiety, could be generated. One hydroxyl radical may abstract the H atom from the C−H bond of the hydrazone group of the second **Pt1** molecule to form a water molecule and another complex radical (A). The slightly slower reaction rate in the water-containing CH_3CN solution versus that in dry acetonitrile (Figure 3) may be related to the release of water in the dark reaction processes. Because of radical coupling between two different complex radicals (A and B), dimerized complex **Pt2** could be formed [route A, third step (B)]. In our preliminary ESI-TOF mass spectrometry analysis of the photoproduct obtained from the photoreaction of **Pt1** in the presence of the well-known radical scavenger butylated hydroxytoluene (BHT; 2,6-di-*tert*-butyl-4-methylphenol),[36] the mass peak (m/z 846) corresponding to BHT-bound **Pt1O** [M_w = 845 (Figure S11 of the Supporting Information)] was observed, suggesting that the photoreaction of **Pt1** involves a radical reaction. Except for **Pt2**, no other dimerized species was observed in this photochemical reaction, suggesting that the selective radical coupling reaction between A and B occurs. Although the reason is under investigation, steric hindrance arising from the two phenyl rings bound to the P atom may play an important role in this radical coupling dimerization reaction. It is well-known that $^1O_2$ shows several interesting reactions for the formation of valuable organic materials, such as endoperoxides from [2+4] cycloadditions, dioxetanes from [2+2] cycloadditions, phosphine oxides from phosphine oxidations, and hydroperoxides from phenol oxidations and "ene" reactions.[37−41] The $^1O_2$-mediated dimerization reaction involving C−N bond formation with **Pt1** is in contrast to the fact that the reactions of organic hydrazines and hydrazones with $^1O_2$ tend to exhibit N−N bond cleavage to form the corresponding ketones/aldehydes and dinitrogen.[37] This would be due to the chelate bonds between the hydrazone ligand and Pt(II) ion; i.e., these bonds suppress N−N bond cleavage in the hydrazone moiety.

On the other hand, a much slower photoreaction of **Pt1** also occurred in a degassed solution as shown in Figure 3, suggesting that other reaction pathways without dissolved dioxygen should exist. UV−vis spectra of the degassed and O_2-saturated CH_3CN solutions were identical in the visible region above 400 nm (see Figure S1 of the Supporting Information), suggesting that the same photoproducts are produced. Our preliminary results for the photoreaction of **Pt1** in H_2O-saturated or dried CH_2Cl_2 solutions (see Figure S12 of the Supporting Information) suggest that water would be the other plausible reactant, because the photoinduced UV−vis spectral change occurred ∼30 times faster in the H_2O-saturated solution than in the dried one (note that both solutions were carefully degassed by Ar bubbling). Although the effect of addition of water on the reaction rate in CH_2Cl_2 was in contrast to that in a CH_3CN solution (as shown in Figure 3), it might be due to the

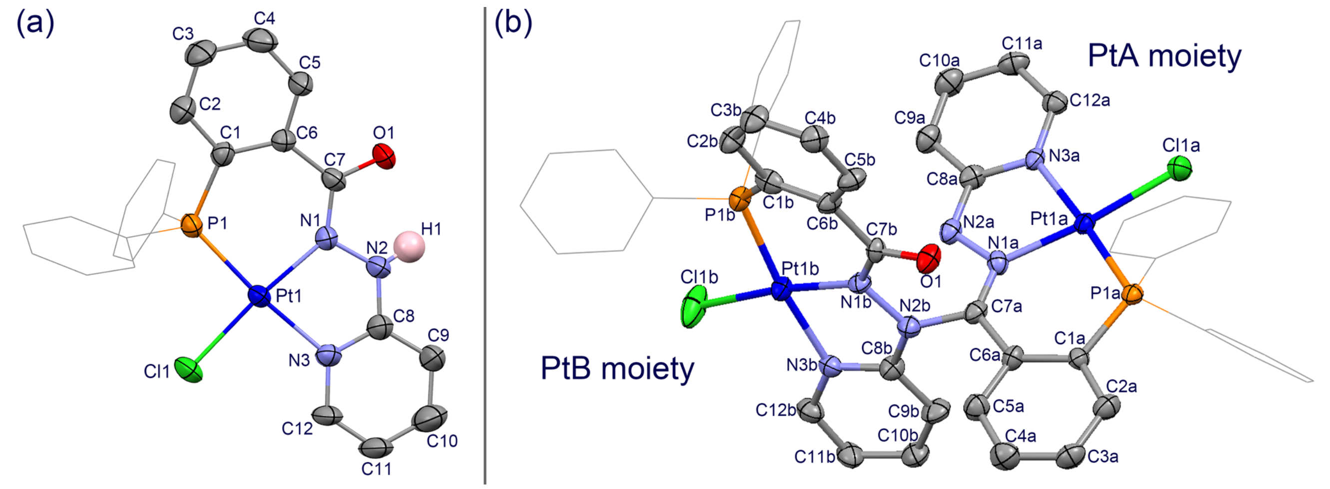

Figure 7. Molecular structures of (a) **Pt1O** and (b) **Pt2** complexes with thermal vibrational ellipsoids at the 50% probability level. Blue, green, orange, red, light blue, and gray ellipsoids and a pink sphere represent Pt, Cl, P, O, N, C, and H atoms, respectively. Hydrogen atoms bound to carbon atoms have been omitted, and phenyl groups bound to phosphorus atoms are drawn as gray line models for the sake of clarity.

Table 2. Selected Bond Lengths (angstroms) and Angles (degrees)

				Pt2	
	HL[a]	Pt1O	Pt1[b]	PtA	PtB
Pt1−Cl1	–	2.297(3)	2.297(3)	2.300(3)	2.295(3)
Pt1−P1	–	2.201(2)	2.220(2)	2.211(3)	2.205(2)
Pt1−N1	–	2.006(7)	1.965(9)	1.996(7)	1.994(7)
Pt1−N3	–	2.079(6)	2.051(7)	2.055(7)	2.059(7)
C6−C7	1.469(15)	1.492(10)	1.469(13)	1.490(13)	1.514(9)
C7−N1	1.280(15)	1.328(9)	1.327(11)	1.314(11)	1.363(11)
N1−N2	1.361(15)	1.389(10)	1.386(11)	1.372(11)	1.424(10)
N2−C8	1.385(17)	1.346(10)	1.355(11)	1.346(11)	1.370(11)
C8−N3	1.337(16)	1.338(11)	1.367(14)	1.362(10)	1.354(11)
C8−C9	1.401(2)	1.402(13)	1.442(14)	1.415(13)	1.401(13)
C7a−N2b	–	–	–	1.455(11)	–
C7−O1	–	1.266(10)	–	–	1.251(11)
C6−C7−N1		122.0(7)	128.85		
N1−N2−C8	118.54(11)	120.7(7)	110.2(8)	113.6(7)	117.6(7)
dihedral angle	25.26	15.18	13.20	6.72	22.05

[a]From ref 23. [b]From ref 20.

difference in solvent polarity. In the weakly polar CH_2Cl_2 solution, the water molecules would form the hydrogen bond with the N atom of the hydrazone moiety of **Pt1** because of the strong proton accepting ability of metal−hydrazone complexes. In such a situation, the photoexcited ILCT state of **Pt1*** with biradical character could react with the hydrogen-bound water to form a hydroxyl intermediate and one $H^\bullet$ radical (route B, first and second steps). The following N−H bond formation between them and the oxidation reaction would produce **Pt1O** [route B, third step (A)]. On the other hand, if the $H^\bullet$ radical reacts with the other ground-state **Pt1**, the complex radical (A) and dihydrogen would be generated. GC analysis for the gas above the photoreaction solution of 0.1 mM **Pt1** with CH_2Cl_2 clearly indicates the evolution of hydrogen gas (see Figure S13 of the Supporting Information). The dimerized complex **Pt2** could be formed by the reaction between the hydroxyl intermediate and the radical (A) and the following oxidation reaction [route B, third step (B)]. Thus, this water-mediated photoreaction may occur in the degassed CH_3CN solution. The fact that the reaction rate in the degassed solution was considerably lower than that in the O_2-saturated one could be due to the fast deactivation of short-lived biradical species of **Pt1*** and/or the weaker hydrogen bonding interaction between **Pt1** and the water molecule in the highly polar CH_3CN than that in the weakly polar CH_2Cl_2.

Crystal Structures of Photoproducts. As discussed above, crystallization of the two photoproducts, **Pt1O** and **Pt2**, was successful. Here, the crystal structure of these complexes is discussed in detail.

Figure 7a shows the molecular structure of **Pt1O**. Selected bond distances and angles are summarized in Table 2. As in **Pt1**, the central Pt ion of **Pt1O** adopts a square-planar coordination geometry, where the four coordination sites are occupied by one chloride, one phosphine, and two nitrogen atoms of the hydrazone ligand, indicating that the Pt center remains in the divalent state. Interestingly, the imine C7 atom was found to be oxygenated, and the C7−O1 distance [1.265(9) Å] was in the typical range for the C═O bond of the carbonyl group. Thus, the imine carbon in the hydrazone moiety was oxidized to form the carbonyl group in the photochemical reaction of **Pt1**. Because of the formation of the carbonyl group, the C6−C7−N1 bond angle is more contracted than that of **Pt1** and is close to the ideal angle of the sp^2 carbon (120°). As expected from the ^{1}H NMR spectrum (Figure 4), the N2 atom in the hydrazone group was protonated and the N1−N2−C8 bond angle is in the typical range for protonated hydrazones. Because of the steric hindrance of the two phenyl groups bound to the phosphorus atom, there was no intermolecular metallophilic interaction between the two Pt ions; however, intermolecular double hydrogen bonds (−N2−H1···O1−C7−) were formed between the two adjacent **Pt1O** molecules.

Figure 7b shows the molecular structure of the other photoproduct, **Pt2**. Complex **Pt2** crystallized in the monoclinic $P2_1/n$ space group. X-ray structural determination clearly revealed that this **Pt2** molecule is composed of two metal−hydrazone complex units linked by the newly formed C−N bond. There are no counter cations or anions, indicating that the dimerized molecule is neutral. In one of the two complex moieties (abbreviated as the **PtA** moiety), the imine carbon atom (C7a) of the hydrazone ligand is bonded to the imine nitrogen atom (N2b) of the adjacent hydrazone moiety (abbreviated as **PtB**). Judging from the C7b−O1 bond distance, another imine carbon atom (C7b) in **PtB** was oxidized to form the carbonyl group, as in the case of **Pt1O**.

These new bond formations considerably affected the hydrazone moieties in the dimerized molecule. For example, the C6−C7, N1−N2, C7−N1, and N2−C8 bond distances in the **PtB** moiety are remarkably longer than those in the **PtA** moiety, whereas the N3−C8 and C8−C9 bond distances in **PtB** are shorter than those in **PtA** and are close to the typical bond lengths in the pyridine ring. It is noteworthy that the longer N1b−N2b bond distance in the **PtB** moiety is very close to the typical distance of a single N−N bond (∼1.45 Å) and the bond length of the newly formed C7a−N2b bond is comparable to the typical distance of a single C−N bond (∼1.47 Å). These bond distances around the N2b atom suggest that the photoinduced dimerization may change the orbital character of the N2b atom from sp^2 to sp^3. In fact, there was a 0.19 Å deviation of the N2b atom from the plane defined by the three adjacent atoms (N1b, C7a, and C8b). Consequently, the N2b atom is the chiral center of this molecule, but two different chiral molecules are mixed in one crystal to form the racemic crystal. In addition, the dihedral angle between the two least-squares planes of the phenylene and pyridine rings in the **PtA** moiety is ∼15° smaller than that in the **PtB** molecule. Because the bond distances and angles of the hydrazone ligand in **PtA** are very close to those in the original (deprotonated) complex **Pt1**, the photoinduced dimerization coupled with oxygenation considerably affected the molecular and electronic structures of **PtB** rather than those of **PtA**. These structural changes mainly observed for the **PtB** moiety suggest that the π electron of the pyridine ring is completely localized in the ring of the **PtB** moiety, though it is delocalized in the hydrazone moiety in **PtA**.

■ CONCLUSION

Evaluation of the photoreactivity of two metal−hydrazone complexes with d^8 metal ions, [NiCl(pbph)] (**Ni1**) and [PtCl(pbph)] (**Pt1**) [Hpbph = 2-(diphenylphosphino)-benzaldehyde-2-pyridylhydrazone], demonstrated an interesting photochemical reaction of **Pt1** in a CH_3CN solution driven by excitation of the ILCT transition to form two different products, whereas the photoreaction of **Ni1** was plausibly precluded by fast deactivation by the lower-lying d−d transition state of the Ni(II) center. In contrast to the photo-oxidation of **HL** to form the phosphine oxide **HL(P═O)** without any change in the hydrazone moiety, single-crystal X-ray structural analyses revealed that a mononuclear Pt(II) complex with the oxygenated hydrazone **Pt1O** and a dinuclear Pt(II) complex with the dimerized hydrazone **Pt2** were formed in the photoreaction of **Pt1**. Changes in the ^{1}H NMR spectral profile under photoirradiation suggested that only two photoproducts were formed in this reaction. In addition, the photosensitized reaction of **Pt1** in the presence of the $^1O_2$-generating photosensitizer MB clearly indicated that the reaction between the reactive $^1O_2$ and ground-state **Pt1** should be involved in this photoreaction. In a highly viscous DMSO solution, **Pt1** was quantitatively converted to mononuclear complex **Pt1O** without the formation of byproducts such as dinuclear **Pt2**. The same **Pt1O** and **Pt2** complexes was also slowly formed in the degassed solution by light irradiation probably because of the other reaction pathway involving the reaction between the photoexcited ILCT transition state of **Pt1*** with the biradical character and H_2O. Further investigation focusing on the steric effect of the hydrazone ligand on the photoreaction is in progress.

■ ASSOCIATED CONTENT

Ⓢ Supporting Information

Changes in the UV−vis spectral profile of **Pt1** in a CH_3CN solution, ESI-TOF mass spectra of **Pt1** and the photoproducts obtained from the photoreaction of a **Pt1**/CH_3CN solution, changes in the ^{1}H NMR spectra of **HL** in a DMSO-d_6 solution under photoirradiation, ^{1}H NMR spectral change of **Pt1** in O_2-saturated CD_3CN and DMSO-d_6 solutions with MB as a photosensitizer, changes in the UV−vis spectral profile and ESI-TOF mass spectra of **Ni1** in a 0.1 mM CH_3CN O_2-saturated solution with 0.01 mM MB, plot of changes in the absorbance of the ILCT band of **Pt1** (λ_{abs} = 530 nm) in a 0.1 mM CH_3CN solution versus photoirradiation time in the presence of DABCO, changes in ^{1}H NMR spectra of **Pt1** in a CD_3CN solution in the presence of dimethyl sulfide under photoirradiation, ESI-TOF mass spectra of the photoproduct obtained from the photoreaction of **Pt1** in a CH_2Cl_2 solution in the presence of 10 equiv of BHT, changes in the UV−vis spectral profile of **Pt1** in a 0.1 mM CH_2Cl_2 H_2O-saturated solution under photoirradiation (λ_{irr} = 529 nm), GC chromatograms of the gas above the photoreaction solution of 0.1 mM **Pt1** and CH_2Cl_2 before (a) and after (b) photoirradiation (λ_{irr} = 529 nm) for 120 min, and the shape of (left) HOMO, (center) LUMO, and (right) LUMO+1 of **Pt1**. This material is available free of charge via the Internet at http://pubs.acs.org.

■ AUTHOR INFORMATION

Corresponding Authors

*E-mail: akoba@sci.hokudai.ac.jp.

*E-mail: mkato@sci.hokudai.ac.jp.

Present Address

‖T.M.: International Institute for Carbon-Neutral Energy Research (WPI-I2CNER), Kyushu University, 744 Motooka, Nishi-ku, Fukuoka 819-0395, Japan.

Notes

The authors declare no competing financial interest.

■ ACKNOWLEDGMENTS

M.K. is grateful to Dr. Yamasaki at Rigaku Corp. for his great contribution to the X-ray analysis in the early stage of this study. This work was supported by Grants-in-Aid for Scientific Research [B (23350025) and C (24550076)], Coordination Programming (2107), Artificial Photosynthesis (2406), Young Scientists [B (24750049)], and the Global COE Program (Project B01, Catalysis as the Basis for Innovation in Materials Science) from MEXT, Japan.

■ REFERENCES

(1) Sawicki, E.; Hauser, T. R.; Stanley, T. W.; Elbert, W. *Anal. Chem.* **1961**, *33*, 93−96.
(2) Shao, J.; Tam, J. P. *J. Am. Chem. Soc.* **1995**, *117*, 3893−3899.
(3) Xiang, Y.; Tong, A.; Jin, P.; Ju, Y. *Org. Lett.* **2006**, *8*, 2863−2866.
(4) Geldard, J. F.; Lions, F. *Inorg. Chem.* **1963**, *2*, 270−282.
(5) Pal, S.; Pal, S. *J. Chem. Soc., Dalton Trans.* **2002**, 2102−2108.
(6) Pelagatti, P.; Bacchi, A.; Carcelli, M.; Costa, M.; Frühauf, H.-W.; Goubitz, K.; Pelizzi, C.; Triclistri, M.; Vrieze, K. *Eur. J. Inorg. Chem.* **2002**, 439−446.
(7) Dawe, L. N.; Thompson, L. K. *Dalton Trans.* **2008**, 3610−3618.
(8) Guo, Y.-N.; Chen, X.-H.; Xue, S.; Tang, J. *Inorg. Chem.* **2012**, *51*, 4035−4042.
(9) Kohata, K.; Kawamonzen, Y.; Odashima, T.; Ishii, H. *Bull. Chem. Soc. Jpn.* **1990**, *63*, 3398−3404.
(10) Chang, M.; Kobayashi, A.; Chang, H.-C.; Nakajima, K.; Kato, M. *Chem. Lett.* **2011**, *40*, 1335−1337.
(11) Mori, A.; Suzuki, T.; Sunatsuki, Y.; Kobayashi, A.; Kato, M.; Kojima, M.; Nakajima, K. *Eur. J. Inorg. Chem.* **2014**, 186−197.
(12) Pelagatti, P.; Bacchi, A.; Balordi, M.; Bolaño, S.; Calbiani, F.; Elviri, L.; Gonsalvi, L.; Pelizzi, C.; Peruzzini, M.; Rogolino, D. *Eur. J. Inorg. Chem.* **2006**, 2422−2436.
(13) Pelagatti, P.; Bacchi, A.; Carcelli, M.; Costa, M.; Fochi, A.; Ghidini, P.; Leporati, E.; Masi, M.; Pelizzi, C.; Pelizzi, G. *J. Organomet. Chem.* **1999**, *583*, 94−105.
(14) Carvalho, M. F. N. N.; Fernandes, T. A.; Galvão, A. M.; Nidda, H.-A. K.; Sampaio, M. A. P. *Inorg. Chim. Acta* **2010**, *363*, 71−76.
(15) Raja, D. S.; Bhuvanesh, N. S. P.; Natarajan, K. *Dalton Trans.* **2012**, *41*, 4365−4377.
(16) Buss, J. L.; Neuzil, J.; Ponka, P. *Arch. Biochem. Biophys.* **2004**, *421*, 1−9.
(17) Zhang, Y.; Zhang, L.; Liu, L.; Guo, J.; Wu, D.; Xu, G.; Wang, X.; Jia, D. *Inorg. Chim. Acta* **2010**, *363*, 289−293.
(18) Green, R. W.; Hallman, P. S.; Lions, F. *Inorg. Chem.* **1964**, *3*, 376−381.
(19) Landge, S. M.; Aprahamian, I. *J. Am. Chem. Soc.* **2009**, *131*, 18269−18271.
(20) Chang, M.; Horiki, H.; Nakajima, K.; Kobayashi, A.; Chang, H.-C.; Kato, M. *Bull. Chem. Soc. Jpn.* **2010**, *83*, 905−910 (the result of TD-DFT calculation of **Pt1** is given in Figure S14 of the Supporting Information).
(21) Ray, D.; Foy, J. T.; Hughes, R. P.; Aprahamian, I. *Nat. Chem.* **2012**, *4*, 757−762.
(22) Kobayashi, A.; Dosen, M.; Chang, M.; Nakajima, K.; Noro, S.; Kato, M. *J. Am. Chem. Soc.* **2010**, *132*, 15286−15298.
(23) Chang, M.; Kobayashi, A.; Nakajima, K.; Chang, H.-C.; Kato, M. *Inorg. Chem.* **2011**, *50*, 8308−8317.
(24) Wong, J. L.; Zady, M. F. *J. Chem. Soc., Chem. Commun.* **1973**, 684−685.
(25) Wong, J. L.; Zady, M. F. *J. Org. Chem.* **1975**, *40*, 2512−2516.
(26) Pervova, I. G.; Melkozerov, S. A.; Slepukhin, P. A.; Lipunova, G. N.; Barachevskii, V. A.; Lipunov, I. N. *Russ. J. Gen. Chem.* **2010**, *80*, 987−993.
(27) Bacchi, A.; Carcelli, M.; Costa, M.; Fochi, A.; Monici, C.; Pelagatti, P.; Pelizzi, C.; Pelizzi, G.; Roca, L. M. S. *J. Organomet. Chem.* **2000**, *593594*, 180−191.
(28) *CrystalClear*; Molecular Structure Corp.: Orem, UT, 2001.
(29) Burla, M. C.; Caliandro, R.; Camalli, M.; Carrozzini, B.; Cascarano, G. L.; De Caro, L.; Giacovazzo, C.; Polidori, G.; Spagna, R. *J. Appl. Crystallogr.* **2005**, *38*, 381−388.
(30) Sheldrick, G. M. *Acta Crystallogr.* **2008**, *A64*, 112−122.
(31) *CrystalStructure version 4.0: Crystal Structure Analysis Package*; Rigaku Corp.: Tokyo, 2000−2010.
(32) DeRosa, M. C.; Crutchley, R. J. *Coord. Chem. Rev.* **2002**, *233*−*234*, 351−371.
(33) Redmond, R. W.; Gamlin, J. N. *Photochem. Photobiol.* **1999**, *70*, 391−475.
(34) Rodgers, M. A. J. *J. Am. Chem. Soc.* **1983**, *105*, 6201−6205.
(35) Nahm, K.; Foote, C. S. *J. Am. Chem. Soc.* **1989**, *111*, 1909−1910.
(36) Fujisawa, S.; Kadoma, Y.; Yokoe, I. *Chem. Phys. Lipids* **2004**, *130*, 189−195.
(37) Landis, M.; Madoux, D. C. *J. Am. Chem. Soc.* **1979**, *101*, 5106−5107.
(38) Bortolus, P.; Monti, S.; Albini, A.; Fasani, E.; Pietra, S. *J. Org. Chem.* **1989**, *54*, 534−540.
(39) Greer, A. *Acc. Chem. Res.* **2006**, *39*, 797−804.
(40) Castro, C.; Dixon, M.; Erden, I.; Ergonenc, P.; Keeffe, J. R.; Sukhovitsky, A. *J. Org. Chem.* **1989**, *54*, 3732−3738.
(41) Clennan, E. L.; Noe, L. J.; Szneler, E.; Wen, T. *J. Am. Chem. Soc.* **1990**, *112*, 5080−5085.